DIAGNOSTYKA, 2025, Vol. 26, No. 4

e-ISSN 2449-5220 **DOI:** 10.29354/diag/214932

ECCENTRICITY MONITORING IN INDUCTION TRACTION MOTORS OF RAILWAY ROLLING STOCK USING THE PRONY METHOD

Sergey GOOLAK ¹, Oleg GUBAREVYCH ^{1,*}, Victor YURCHENKO ¹, Oleksandr POHOSOV ², Vasyl SAVYK ³

*Corresponding author, e-mail: oleg.gbr@ukr.net

Abstract

The problems of improving and perfecting the diagnostic systems of railway transport drives continue to be the most relevant. The article proposes a method for operational monitoring of rotor eccentricity in induction traction motors of railway transport. Eccentricity is an indicator of defects that can be detected at the early stages of operation. The developed diagnostic system combines the Prony method and the Wiener–Hopf theorem, which allows to increase the accuracy of spectral analysis of stator phase currents in conditions of noise and alternating modes. The simulation modeling of the CTA-1200 traction motor of the DS-3 electric locomotive drive showed that the Prony method provides more accurate detection of subsynchronous type harmonics compared to the traditional fast Fourier transform. The obtained symmetrical spectral components reduce the risk of erroneous interpretation. The presented approach has confirmed its effectiveness for increasing the reliability of traction motor diagnostics.

Keywords: diagnostics, monitoring, induction motor, traction drive, field-oriented control, eccentricity, Prony method, Wiener-Hopf theorem.

1. INTRODUCTION

When building a system for operational diagnostics of monitoring the condition of traction drive elements, the features of the traction system of railway rolling stock should be taken into account.

Traction systems of railway rolling stock can be classified by: types of traction motors, organization of the power supply system, organization of the control system.

Thus, as traction motors on vehicles, direct and pulsating current motors [1, 2], induction motors [3, 4] and synchronous motors with permanent magnets [5, 6] are used.

Traction drives of railway rolling stock can be powered from the contact network (electric rolling stock) [7, 8], diesel generator set (thermal locomotives) [9, 10] and from a hybrid power system, i.e. when using on-board energy storage devices [11-13].

The following systems are used as traction drive control systems for railway rolling stock: scalar system [14, 15], field-oriented system [16] and direct torque control [17, 18].

In addition to the structural features of the traction drive, when building a diagnostic system, it is necessary to take into account various disturbances that act on the traction drive during the operation of railway rolling stock. Such disturbances include a constant change in the dynamics of the rolling stock [19-21]. Changing the dynamics of the rolling stock leads to a change in the load of the traction motors. This fact affects the accuracy of determining diagnostic symptoms [22].

In addition, during the operation of the rolling stock, the speed of movement changes all the time. This leads to a change in the frequency of rotation of the motor shaft. This circumstance leads to the appearance of quasi-symmetrical modes of operation of the traction drive [23]. In addition, this also complicates the operation of the diagnostic system as part of the traction drive.

In traction drives of railway rolling stock, induction motors occupy a dominant place. Therefore, it was quite logical and expedient to choose an induction traction motor as the object of research.

Received 2025-10-02; Accepted 2025-12-01; Available online 2025-12-02

¹ Department of Electromechanics and rolling stock of railways of Educational and Scientific Kyiv Institute of Railway Transport, National Transport University (01010), Ukraine

² Department of Heat Engineering, Kyiv National University of Construction and Architecture (03307), Ukraine ³ Department of Oil and Gas Engineering and Technologies of the National University "Yuriy Kondratyuk Poltava Polytechnic" (36011), Ukraine

^{© 2025} by the Authors. Licensee Polish Society of Technical Diagnostics (Warsaw. Poland). This article is an open access article distributed under the terms and conditions of the Creative Commons Attribution (CC BY) license (http://creativecommons.org/licenses/by/4.0/).

In [24], a systematization of damage to an induction motor was carried out. In the same work, it was shown that current, thermal and vibration diagnostic methods can be used to diagnose the presence of defects in an induction motor.

Vibration diagnostic methods [25, 26] are effective in building bench diagnostics. When building operational diagnostics, they are ineffective, since the traction drive is affected by vibrations caused by operational factors.

Temperature diagnostic methods [27, 28] are effective, but less accurate than vibration and current methods.

In [29], the effectiveness of current methods in diagnosing interturn short circuits in the stator windings of an induction motor is shown, in [30] in diagnosing interturn short circuits and the state of insulation in the stator windings of an induction motor, and in [31] in diagnosing defects in the rotor of an induction motor.

When diagnosing the presence of defects in an induction motor as part of a traction drive, another difficulty arises. This difficulty is associated with the quality of the supply voltage supplied to the induction motor from an autonomous voltage inverter [32]. The asymmetry of the resistances in the autonomous inverter leads to the asymmetry of the supply voltage system of the induction motor. Diagnostic symptoms in the case of asymmetry of the supply voltage system are similar to the diagnostic symptoms of damage to the stator and rotor windings of an induction motor [33, 34].

The principles of building a system for monitoring the condition of the stator windings in a traction drive with possible asymmetry of the supply voltage system are given in [23]. Since the diagnosis of the presence of defects in the stator windings is performed in a traction drive with field-oriented control, it becomes possible to apply additional diagnostic symptoms - phase flux linkages of the stator. In [23], it is proposed to diagnose asymmetric emergencies by simultaneously analyzing the nature of changes in the values of phase flux linkages and stator currents. Despite the obviously correct approach to solving the problem, [23] did not investigate the impact of load changes on the efficiency of the diagnostic system. In [35], it is proposed to use rotor slip as a diagnostic symptom when building a system for monitoring the condition of the rotor windings. The proposed solution turned out to be effective in determining a defect in the rotor windings. However, the slip value also depends on the load of the induction motor. In [35], as in [23], the influence of load changes on the efficiency of the diagnostic system was also not investigated.

A number of defects indicated in [24] lead to the appearance of rotor eccentricity, which is the most common mechanical defect of an induction motor. In [36], it is stated that such a defect as eccentricity accounts for up to 40% of induction motor failures. Monitoring the appearance of rotor eccentricity and identifying its nature is currently the most relevant and

difficult task in diagnosing the condition of induction motors.

Eccentricity leads to:

- one-sided magnetic attraction;
- rotor engagement with the stator;
- increased wear of bearings.

The causes of eccentricity are different, but they lead to similar negative consequences.

The causes of eccentricity are:

- poor-quality manufacturing or repair of the motor;
- operational factors, as a result of which the geometry of the motor design is disturbed;
- bearing wear;
- shaft deflections, etc.

In the presence of this type of defect, it is possible to continue operating the motor. At the same time, the presence of eccentricity leads to a decrease in the reliability and durability of the induction motor. A decrease in reliability leads to a decrease in the technical, economic and operational parameters of the induction motor.

As noted above, when operating an induction motor with eccentricity, a one-sided magnetic attraction is created, which affects the reduction of efficiency, the increase in the heating temperature of the induction motor and the reduction of the starting torque. As a result of the one-sided magnetic attraction, additional higher harmonics arise, which affect a number of electromagnetic parameters of the motor [37, 38]. Eliminating the above-mentioned negative consequences of the presence of eccentricity by timely detection of this defect at an early stage is an important

In works devoted to the study of diagnosing the presence of eccentricity, two of its types are considered: static and dynamic. Static eccentricity is a shift of the axis of rotation of the motor shaft relative to the stator package bore. The reasons for its appearance are:

- load imbalance;
- vibrations;
- shaft misalignment;
- sharp change in load and overload;
- bearing failure, etc.

Dynamic eccentricity – displacement of the axis of the outer surface of the rotor relative to the axis of its rotation. This type of eccentricity is accompanied by rotor beating, which occurs due to the forces of onesided magnetic attraction as a result of poor-quality repair or manufacturing defects.

The value of dynamic eccentricity is much less than static. Dynamic eccentricity is not of decisive importance for determining the current diagnosis of the motor condition. That is why it is advisable to conduct research on static eccentricity indicators, which carry more diagnostic information.

Another important aspect when building a system for operational diagnostics of the presence of eccentricity is the choice of a method for processing diagnostic information [36]. Diagnostic symptoms when building a functional diagnostic system are [36]:

- rotor slot passage harmonics (RSH);

- lateral harmonics of the rotor around the supply frequency;
- doubled supply frequency and lateral harmonics around it.

In the presence of eccentricity in the signals of the stator phase currents, the amplitudes of the RSH harmonics change [39-41]. The amplitudes of the RSH harmonics are functions of the amplitudes of the stator phase currents, the frequency of the supply voltages, the slip and the modulation coefficient of the eccentricity, which is directly proportional to the degree of eccentricity. In addition, the phase currents of the stator are affected by noise caused by the heating of the stator windings of the induction motor. When building a system for operational diagnostics of the presence of eccentricity, difficulties arise due to the constant change in the frequency of the motor supply voltage and the presence of thermal noise.

A comparison of diagnostic information processing methods when building a system for monitoring the presence of eccentricity in IMs is given in [36].

Such methods include:

- the method of analysis of the current signatures of the electric motor (MCSA) [42-44];
- methods of tracking harmonics of order (HOTA) [45, 46];
- parametric methods (MUSIC, ESPRIT) [47-49];
- methods based on Park vectors [50-52];
- the Prony method [53-55];
- artificial intelligence methods [56-58];
- fractional moment statistics [59-61].

From the comparison of these methods, it follows that the most effective method for detecting the presence of eccentricity by an operational diagnostic system is the Prony method, the advantages of which are [36]:

- short signal sampling;
- absence of the spectral leakage effect;
- low sampling frequency.

However, the Prony method has a number of disadvantages, including:

- complex signal processing;
- no criteria for selecting the model order.

In this paper, it is proposed to use the Prony method, supplemented by an algorithm for implementing the Wiener-Hopf theorem, when conducting operational monitoring of the presence of eccentricity in the work of an IM.

2. ADAPTATION OF THE PRONY METHOD FOR ANALYSIS OF DIAGNOSTIC INFORMATION WHEN CONSTRUCTING AN OPERATING SYSTEM FOR DIAGNOSTIC OF THE PRESENCE OF ROTOR ECCENTRICITY IN TRACTION IMS

From the analysis of the advantages and disadvantages of the Prony method (Section 1) when applying it to process diagnostic information when monitoring the presence of eccentricity in IMs, it follows that the lack of criteria for selecting the order of the model is the most significant disadvantage.

2.1. Basic algorithm of the Prony method

The Prony method is one of the classical approaches to approximating signals by a sum of exponents, which allows recovering the parameters of harmonic components based on a limited number of samples. This method is widely used for the analysis of damped oscillations and spectrum structures in conditions of limited data volume. The steps of the Prony procedure for preparing k exponents for 2k data samples are:

At the first step, the coefficients of the polynomial of the following equation are found [62]:

$$\begin{bmatrix} i_{s}[k] & i_{s}[k-1] & \dots & i_{s}[1] \\ i_{s}[k+1] & i_{s}[k] & \dots & i_{s}[2] \\ \vdots & \vdots & \dots & \vdots \\ i_{s}[2k-1] & i_{s}[2k-2] & \dots & i_{s}[k] \end{bmatrix} \\ \cdot \begin{bmatrix} a[1] \\ a[2] \\ \vdots \\ a[p] \end{bmatrix} = \begin{bmatrix} i_{s}[k+1] \\ i_{s}[k+2] \\ \vdots \\ i_{s}[2k] \end{bmatrix},$$
(1)

where k – the order of the model;

 $i_s[p]$ – the stator phase current counts;

a[p] – the coefficients of the polynomial.

At the second step, the roots of the polynomial are determined, which is determined by equation [62]:

$$\varphi(z) = \prod_{i=1}^{k} (z - z_i) = \sum_{n=0}^{k} a[n] \cdot z^{k-n} = 0,$$
(2)

where z_i – the roots of equation (2).

The roots of the polynomial z_i are necessary to form the elements of the matrix of the equation [62]:

$$(Z^H \cdot Z) \cdot h = (Z^H \cdot x), \tag{3}$$

where the $(M \times k)$ -matrix **Z**, $(k \times 1)$ -vector **h** and $(M \times 1)$ -vector of data counts **x** determined as [62]:

$$Z = \begin{bmatrix} 1 & 1 & \cdots & 1 \\ z_1 & z_2 & \cdots & z_p \\ \vdots & \vdots & \vdots & \vdots \\ z_1^{N-1} & z_2^{N-1} & \cdots & z_p^{N-1} \end{bmatrix};$$

$$h = \begin{bmatrix} h_1 \\ h_2 \\ \vdots \\ h_p \end{bmatrix}; \quad x = \begin{bmatrix} i_s[1] \\ i_s[2] \\ \vdots \\ i_s[p] \end{bmatrix}, \tag{4}$$

where M – the number of stator phase current counts $i_s[1], ..., i_s[M]$

The Hermitian $(k \times k)$ -matrix $\mathbf{Z}^H \cdot \mathbf{Z}$ has the form [62]:

$$Z^{H} \cdot Z = \begin{bmatrix} \gamma_{11} & \dots & \gamma_{1k} \\ \vdots & \vdots & \vdots \\ \gamma_{k1} & \dots & \gamma_{kk} \end{bmatrix}, \tag{5}$$

where:

$$\gamma_{ji} = \sum_{n=0}^{M} \left(z_j^* \cdot z_i \right)^n = \gamma_{ij}. \tag{6}$$

Below is the relation that allows avoiding the addition operation in expression (6). It has the following form [62]:

$$\gamma_{ji} = \begin{cases} \frac{\left(z_{j}^{*} \cdot z_{i}\right)^{M} - 1}{\left(z_{j}^{*} \cdot z_{i}\right) - 1}, & z_{j}^{*} \cdot z_{i} \neq 1; \\ N, & z_{i}^{*} \cdot z_{k} = 1. \end{cases}$$
(7)

Usually, in practice, the number of data samples M exceeds the minimum number required to fit a model with k exponents, i. e. M > 2k. In this conditional case,

the sequence of data samples can only be approximated as an exponential sequence [62]:

$$\hat{i}[m] = \sum_{i=1}^{k} h_i \cdot z_i^{m-1}, \tag{8}$$

where $1 \le m \le M$.

The sum of squares of the error $\varepsilon[k]$ is determined as in [62]:

$$\rho[k] = \sum_{m=1}^{M} |\varepsilon[m]|^2 = \sum_{m=1}^{M} |i_s[m] - \hat{\imath}_s[m]|^2 =$$

$$= \sum_{m=1}^{M} |i_s[m] - \sum_{i=1}^{k} h_i \cdot z_i^{m-1}|^2, (9)$$

In the presence of a significant level of additive noise, the Prony method doesn't give satisfactory results. This is due to the fact that under such conditions, the specified method does not allow taking into account the presence of "non-white" noise in the process being analyzed. When the Prony method is used in the presence of strong additive noise, very inaccurate estimates of the damping coefficients are obtained, the values of which often exceed their true values [62].

2.2. Justification of the criterion choice for determining the order of the Prony model

There are many different criteria for choosing the order of AR-models – a kind of objective functions. Two similar criteria were proposed by Akaike [63]. The first of them is the final prediction error (FPE). According to this criterion, the choice of the order of the AR-process is carried out in such a way as to minimize the average variance of the error at each step of the prediction. In this criterion, the prediction error is the sum of the powers in the unforeseen part of the analyzed process and as a certain value that characterizes the inaccuracy of the estimation of ARparameters. FPE for the AR-process is determined using the expression [63]: $FPE[k] = \hat{\rho}_k \cdot \left(\frac{M + (k+1)}{M - (k+1)}\right),$

$$FPE[k] = \hat{\rho}_k \cdot \left(\frac{M + (k+1)}{M - (k+1)}\right),\tag{10}$$

where N – number of data samples;

p – order of the AR-process;

 $\hat{\rho}_k$ - the estimated value of the dispersion of "white noise" (which is used as the linear prediction error).

As the order k increases, the value of the component in parentheses increases. This characterizes the increase in the estimation uncertainty $\hat{\rho}_k$ for the dispersion of the FPE. The value of k is chosen from the condition of the minimum value of the FPE. For ideal AR processes, the FPE criterion provides excellent results, but for real signals this criterion turns out to be too conservative and leads to the choice of an underestimated model order k. The maximum likelihood method is the basis of the second Akaike criterion, which is called the Akaike information criterion (AIC). According to this criterion, the order of the model is determined by minimizing some information-theoretic function. For the case when the AR process under study has Gaussian statistics, the AIC will be determined as [64]:

$$AIC[k] = M \cdot ln(\hat{\rho}_k) + 2 \cdot k. \tag{11}$$

Term 2k characterizes the cost of using additional AR-coefficients, but this doesn't lead to a significant

reduction in the prediction dispersion error. And in this case, the model order k is chosen from the condition of the minimum value of the AIC. For $M \rightarrow \infty$, the first and second Akaike criteria are asymptotically equivalent. If the data don't correspond to AR-processes, when applying AIC, the model order k turns out to be significantly underestimated [66].

In [65] it is stated that the IKA is a statically unsound criterion for $M \rightarrow \infty$. This is due to the fact that in this case, when choosing the correct order of the model, the probability of error doesn't tend to zero. This leads to an overestimation of the model order value in the case when the length of the data record increases. To eliminate this drawback, in [68] another AIC variant is proposed, which has the following form [66]:

$$MDL[k] = M \cdot ln(\hat{\rho}_k) + k \cdot ln(M),$$
 (12)

where MDL - the minimum description length, which can be said to be statically robust, since the value $k \cdot ln(M)$ increases faster with increasing M than in the case of k.

A third choice of criterion in [67] was called the autoregressive transfer function criterion (AFTC). In this case, the order of the model p is chosen equal to the order at which the estimate of the difference in mean square error between the true error prediction filter (which may be infinite in length) and the filter being estimated is minimal. This difference can be calculated, even with an unknown filter prediction of the true error [66]:

$$AFTC[k] = \left(\frac{1}{M} \cdot \sum_{j=1}^{k} \bar{\rho}_{j}^{-1}\right) - \bar{\rho}_{k}^{-1}, (13)$$

where $\bar{\rho}_j = [M/(N-1)] \cdot \hat{\rho}_j$.

And in this case, k is chosen from the condition of the minimum value of the AFTC[k].

The results of signal spectrum evaluation using the FPE, AIC and AFTC criteria differ little from each other, especially in the case of real signals, rather than simulated AR processes. In [68] it is shown that in the case of short data records, none of these criteria provides satisfactory results. For harmonic processes in the presence of noise, the use of FPE and AIC leads to an underestimate of the model parameter, especially in cases where the signal/noise ratio is large. In connection with this fact, it is proposed to use AFTC for model order selection.

2.3. Algorithm for implementing the Wiener-Hopf theorem

In conditions of a significant level of additive noise, to ensure satisfactory results, the correct choice of the model order is proposed to be carried out by applying the Wiener-Hopf theorem to the input signals (phase stator currents).

For discrete values of stator phase currents, the Wiener-Hopf theorem can be applied as [69]:

$$\begin{cases} K_{I_{S}}(t-pT,t-mT) = \\ = \sum_{i=0}^{M_{1}} \sum_{j=0}^{M_{2}} c_{i,j} \cdot K_{I_{S},n}(t-(p-i) \cdot T,t-(m-j) \cdot T), \\ k \in M_{1}, \quad n \in M_{2}, \end{cases}$$

(14)

where $K_{Is}(t-p\cdot T, t-m\cdot T)$ – the function of mutual correlation of the stator phase current and noise;

 $K_{Is,n}(t-(p-i)\cdot T, t-(m-j)\cdot T)$ – the autocorrelation function of the stator phase current.

Determining all unknowns $y_{i,j}$ in equation (14) allows us to find an impulse function that minimizes the mean square errors of filtering the random value of the stator phase current.

Then the stator phase current after applying the Wiener-Hopf theorem is defined as [69]:

$$i_s'(n) = \sum_{i=0}^{N_1} \sum_{j=0}^{N_2} c_{i,j} \cdot i_s((n-i)-j).$$
(15)

2.4. Determination of the Prony spectrum

The Prony spectrum is determined for the values of the exponential approximation $\hat{i}_s[m]$, not for the values of the original time sequence is[m].

In determining the Prony spectrum, a two-sided function of the form [62] was used

$$\hat{i}_{s}[m] = \begin{cases} \sum_{k=1}^{k} h_{k} \cdot z_{k}^{m}, & m \ge 0; \\ \sum_{i=1}^{k} h_{i} \cdot (z_{i}^{*})^{-m}, & m < 0, \end{cases}$$

$$e \quad z_{i} = exp(\alpha_{i} \cdot T + j2 \cdot \pi \cdot f_{i} \cdot T) \quad \text{and} \quad z^{*}_{i} = exp(-1)$$

 $\alpha_i \cdot T + j2 \cdot \pi \cdot f_i \cdot T$). This definition ensures the symmetry of the decaying part of the exponent with respect to the origin. Function (35) has the following z-transform [62]

$$\hat{I}_{s}[m] = \sum_{i=1}^{k} h_{i} \cdot \left(\frac{1}{1 - z_{i} \cdot z^{-1}} - \frac{1}{1 - (z_{i}^{*} \cdot z)^{-1}} \right) \\
= \sum_{i=1}^{k} h_{i} \cdot \left(\frac{\left(z_{i} - \frac{1}{z_{i}^{*}} \right) \cdot z^{-1}}{1 - \left(z_{i} + \frac{1}{z_{i}^{*}} \right) \cdot z^{-1} + \left(\frac{z_{i}}{z_{i}^{*}} \right) \cdot z^{-2}} \right), \tag{17}$$

and converges for $||z_i|| \le |z| \le |1/z_i|$. If also assumed that $|z_i| < 1$, and use the substitution $z = exp(i2 \cdot \pi \cdot f \cdot T)$ for expression (36), then the discrete-time Fourier transform (DTFT) will have the form [62]:

$$\hat{I}_{s}[m] = T \cdot \hat{X}_{2}(exp[j2 \cdot \pi \cdot f \cdot T]) = \\
= \sum_{i=1}^{k} h_{i} \cdot \\
\left(\frac{T \cdot (exp[\alpha_{i} \cdot T] - exp[-\alpha_{i} \cdot T]) \cdot exp[j2 \cdot \pi \cdot \{f_{i} - f\} \cdot T]}{1 - (exp[\alpha_{i} \cdot T] + exp[-\alpha_{i} \cdot T]) \cdot exp[j2 \cdot \pi \cdot \{f_{i} - f\} \cdot T] + exp[j2 \cdot \pi \cdot \{f_{i} - f\} \cdot T]}\right)$$
(18)

where α_i – the *i*-th damping coefficient; f_i – the frequency of the *i*-th sinusoid;

T – the signal period.

The *i*-th gamping according to the expression [62]: $\alpha_i = \frac{\ln[z_i]}{T}, s^{-1}.$ The *i*-th damping coefficient is determined

$$\alpha_i = \frac{\ln[z_i]}{T}, s^{-1}. \tag{19}$$

The frequency of the *i*-th sinusoid is determined as [62]:

$$f_i = \frac{arctg\left[\frac{Re(z_i)}{Im(z_i)}\right]}{2 \cdot \pi \cdot T}, Hz.$$
 (20)

The signal period is determined according to the expression [62]:

$$T = \frac{1}{f_c}. (21)$$

 $T = \frac{1}{f_s}.$ (21) In equations (19)-(21) z_i - the *i*-th root of the characteristic equation, f_s – frequency of the supply voltage of the IM.

3. DEVELOPMENT OF A STRUCTURAL SCHEME FOR MONITORING THE PRESENCE OF ECCENTRICITY

3.1. Algorithm of operation of the eccentricity monitoring scheme

The algorithm of the rotor eccentricity monitoring scheme is shown in Fig. 1. To implement the Prony method algorithm, the number of stator phase current signal samples N is selected (Unit 1). The Wiener-Hopf theorem is applied to the stator phase current signals input from the corresponding current sensors (Unit 2) in order to reduce the additive noise level (Unit 3). Equations (14)-(15) are implemented in Unit 3.

In [62], it is shown that the initial order of the model is recommended to be chosen from the interval $M/3 \le i \le M/2$. The initial order of the model i=M/2 is selected (Unit 4).

In Unit 5, the roots of the characteristic equation z_i are calculated for the selected model order (equations (1) and (2) are implemented). The coefficients of the impulse function h_i are calculated from the calculated roots of the characteristic equation in accordance with expressions (3)-(7). (Unit 6).

Equations (8)-(9) are implemented in Unit 7, where the sum of squares of the error is determined. Based on the calculated sum of squares of the error in Unit 8, the autoregressive transfer function of the criterion (AFTC) is calculated (13). In Unit 9, the minimum value of AFTC[k], which is the order of the model, is found.

If the sample number of the stator phase current signal is greater than M, in Unit 10, the roots of the characteristic equation z_i are calculated for the selected model order (equations (1) and (2) are implemented). Based on the calculated roots of the characteristic equation in accordance with expressions (3)-(7), the coefficients of the impulse function hi are calculated. (Unit 11).

In unit 12, the k-th damping coefficient α_k and the frequency of the k-th sinusoid f_k are determined (expressions (19)-(20)). According to the calculated values of the i-th damping coefficients αk and the frequencies of the i-th sinusoids in Unit 13, the components of the amplitude-frequency spectrum (AFS) of the stator phase current are calculated based on equation (18).

In the presence of eccentricity, both the stator phase current and the magnetic flux contain subsynchronous components [36]. The frequencies of these components are determined as [36]: $f_{sbh} = f_s \pm n \cdot f_r$; n = 1,2,3,...,

$$f_{shh} = f_s \pm n \cdot f_r; \quad n = 1, 2, 3, ...,$$
 (22)

where f_s – frequency of the supply voltage of the IM; f_r – frequency of subsynchronous harmonics, which is determined as [36]: $f_r = f_s \cdot \frac{1-s}{p},$

$$f_r = f_s \cdot \frac{1-s}{p},\tag{23}$$

where p – the number of pole pairs; s – the rotor slip.

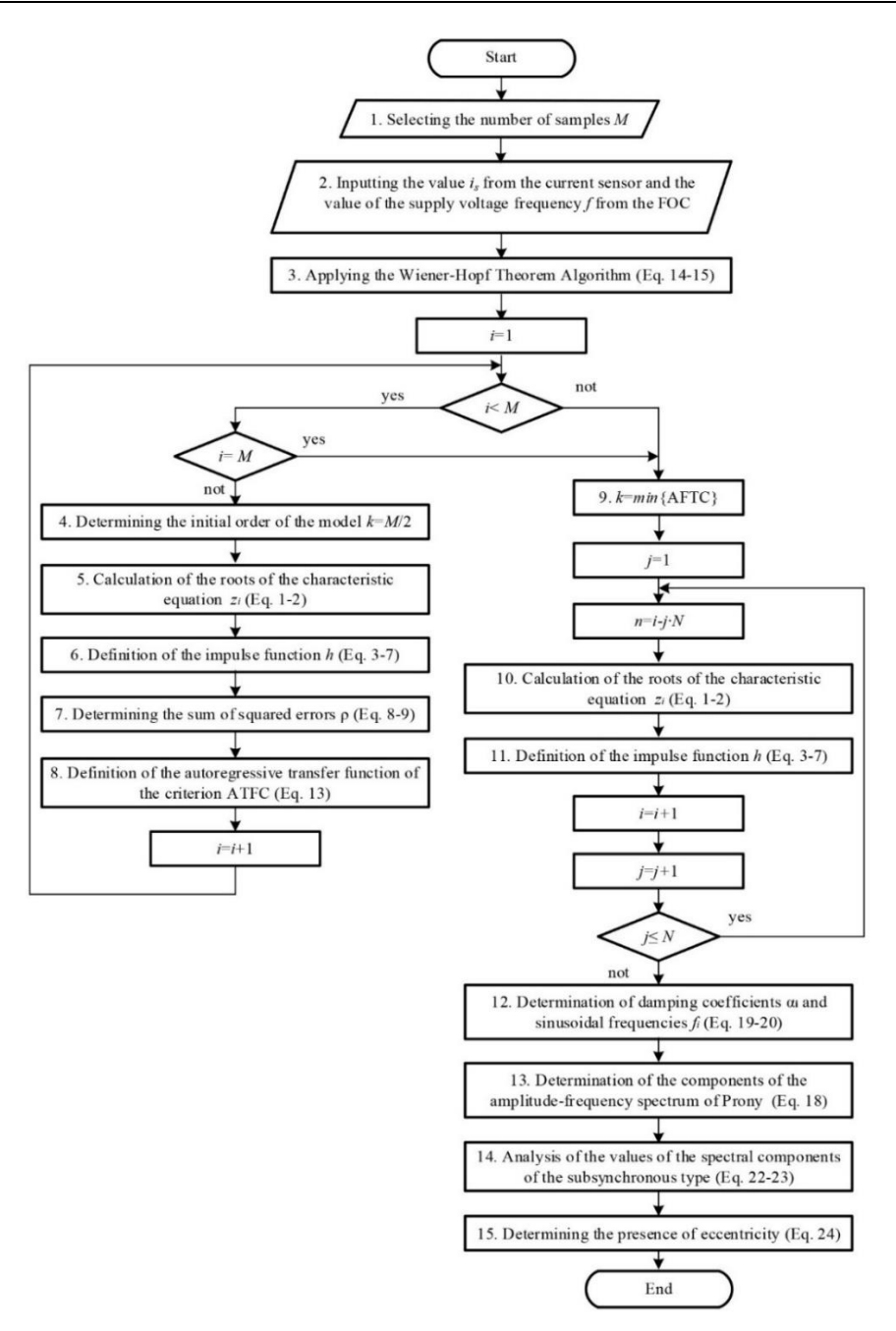


Fig. 1. Functioning algorithm of the rotor eccentricity monitoring scheme

In the presence of eccentricity, the stator phase current is determined as [36]:

$$\begin{split} I_{ecc}[n] &= I_m \cdot \left(1 + \gamma \cdot cos(2 \cdot \pi \cdot f_r \cdot \Delta t \cdot n + \varphi_0)\right) \cdot \\ &\quad \cdot cos(2 \cdot \pi \cdot f_s \cdot \Delta t \cdot n), (24) \end{split}$$

where $I_{ecc}[n]$ – the value of the phase current stator of an IM in the presence of eccentricity;

 γ -the eccentricity modulation coefficient, which is directly proportional to the degree of eccentricity; ϕ_0 - the stator current phase.

In block 14, based on the calculated components of the amplitude-frequency spectrum and in accordance with expressions (22) and (24), the presence of subsynchronous type harmonics is analyzed. In the presence of subsynchronous type harmonics, the degree of eccentricity α is determined in block 15. If $\gamma \ge 10\%$, a decision is made on the impossibility of further operation of the induction motor.

3.2. Structural diagram of monitoring the presence of eccentricity

The block diagram of the eccentricity monitoring Unit and its inclusion in the TD with FOC of IMs is shown in Fig. 2.

The phase currents of the stator of the IM i_{cA} , i_{cB} and i_{cC} comes from the current sensors, and the frequency of the supply voltage IM f_s comes from the FOC to the Unit "Applying the Wiener-Hopf Theorem Algorithm". The algorithm of the Wiener-Hopf theorem is implemented in this Unit.

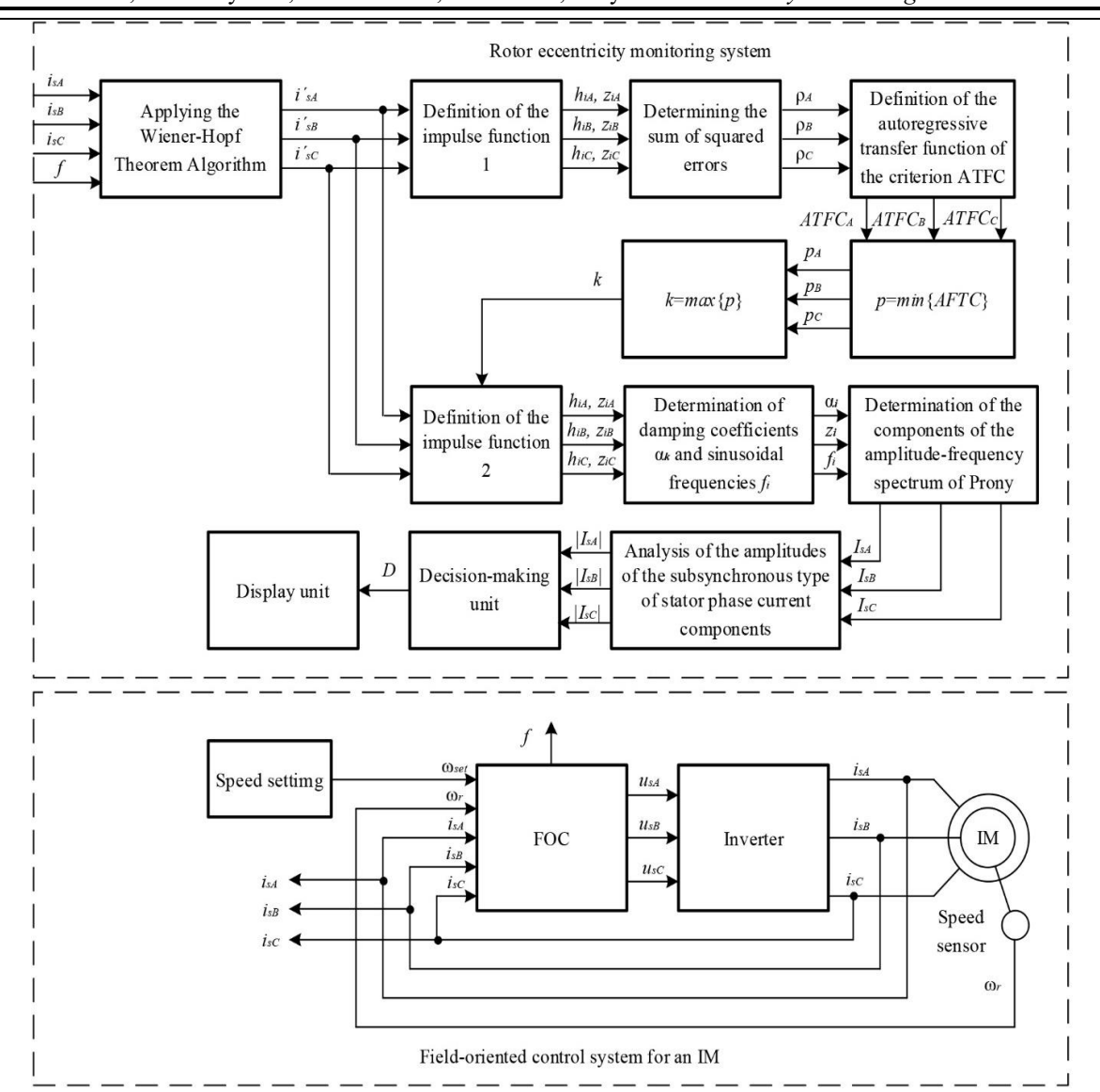


Fig. 2. Block diagram of the eccentricity monitoring unit

The signals of the phase currents of the stator of the induction motor i'_{sA} , i'_{sB} and i'_{sC} from the output of the Unit "Applying the Wiener-Hopf Theorem Algorithm" are fed to the Units "Determination of the impulse function 1" and "Determination of the impulse function 2". In accordance with the algorithm of the circuit operation (Fig. 1), the Unit "Determination of the impulse function 1" is included when the number of samples of the stator phase current signals is $n \le N$, and the Unit "Determination of the impulse function 2" is included when n > N.

In Units "Determination of the impulse function 1" and "Determination of the impulse function 2", the roots of the characteristic equation z_{iA} , z_{iB} , z_{iC} and the coefficients of the impulse characteristic h_{iA} , h_{iB} , h_{iC} are determined. Signals z_{iA} , z_{iB} , z_{iC} and h_{iA} , h_{iB} , h_{iC} from the output of the Unit "Determination of the impulse function 1" are fed to the block "Determination of the sum of squared errors" where estimates of the stator phase current signals $\hat{\iota}_{SA}$, $\hat{\iota}_{SB}$, $\hat{\iota}_{SC}$ are determined, on the basis of which the sums of squared errors $\hat{\rho}_A$, $\hat{\rho}_B$, $\hat{\rho}_C$ are calculated. Based on the signals $\hat{\rho}_A$, $\hat{\rho}_B$, $\hat{\rho}_C$ in the block "Determination of the autoregressive transfer

function of the criterion ATFC" the autoregressive transfer functions of the criterion ($ATFC_A$, $ATFC_B$, $ATFC_C$) are determined. In the block « $p=min\{AFTC\}$ » the minimum values of the autoregressive transfer functions of the criterion p_A , p_B , p_C are determined. In the Unit " $k=max\{p\}$ " the maximum value among the signals k_A , k_B , k_C is determined. This value is the order of the model p.

In the Unit "Determination of the impulse function 2" for the calculated equation z_{iA} , z_{iB} , z_{iC} and the coefficients of the impulse response h_{iA} , h_{iB} , h_{iC} are determined. The signals z_{iA} , z_{iB} , z_{iC} and h_{iA} , h_{iB} , h_{iC} from the output of the Unit "Determination of the impulse function 1" are fed to the Unit "Determination of damping coefficients α k and sinusoidal frequencies f_i " where the i-th damping coefficients α_i and the frequency of the i-th sinusoid f_i are determined

Based on the signals h_{iA} , h_{iB} , h_{iC} , α_i and f_i , the components of the AFS of the stator phase current signals I_{sA} , I_{sB} , I_{sC} are calculated in the Unit "Determination of the components of the amplitude-frequency spectrum of Prony", and in the Unit "Analysis of the amplitudes of the subsynchronous type

of stator phase current components" the presence of subsynchronous type harmonics, their frequencies f_{sbhA} , f_{sbhB} , f_{sbhC} and amplitudes $||I_{sA}|$, $|I_{sB}|$, $|I_{sC}|$ are determined. In the presence of subsynchronous type harmonics, the degree of eccentricity γ is determined according to their specified parameters in the Unit "Decision-making unit". When the value of γ <10%, the signal D=0 is received by the information display system (Unit "Display unit"). This indicates that the value of the rotor eccentricity is within the permissible limits. When $\gamma \ge 2\%$, the information display system (the "Display unit" Unit) receives a signal D=1. This indicates that the value of the rotor eccentricity exceeds the permissible limits.

4. MODELING RESULTS AND DISCUSSION

4.1. Justification of the choice of the object of study

On the railways of Ukraine, mainline electric locomotives of alternating current with induction traction motors of the DS-3 series are operated. The TD of these electric locomotives use FOC. It is the TD of the DS-3 electric locomotive that was chosen as the object of study.

On the DS-3 electric locomotive, IM of the STA-1200 series are used as traction motors, the parameters of which are given in Table 1 [70, 71].

4.2. Modeling results

A simulation model of the TD of the DS-3 electric locomotive is given in [16], therefore it is not given in this work. In order to simplify the research in the model [16], the inverter was replaced by a sinusoidal system of supply voltages, the sinusoids of which are formed by a field-oriented control scheme. The model given in [16] is supplemented with a block "System for monitoring the presence of rotor eccentricity" in accordance with Fig. 2. To take into account thermal noise in the TD, the model is supplemented with a source of "white noise". The noises were superimposed on the sinusoids of the supply voltages of the induction motor.

When modeling, the signal/noise ratio was selected as SNR=30 dB. SNR determines the maximum noise amplitude, according to the expression [36]:

$$SNR = 20 \cdot log_{10} \left(\frac{I_m}{I_n} \right) \Rightarrow$$

$$\Rightarrow I_n = \frac{I_m}{10^{\frac{SNR}{20}}} = \frac{636.4}{10^{\frac{30}{20}}} = 17.8, A \qquad (25)$$

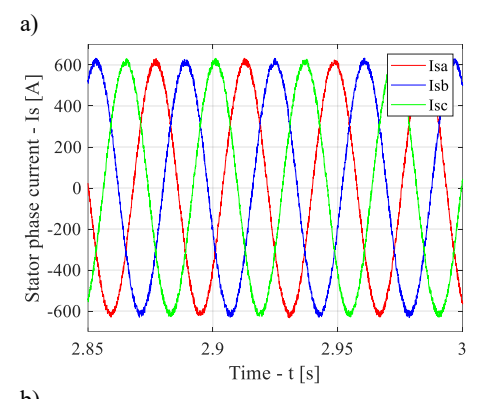
The simulation was carried out at the nominal (n_{rnom}) , reduced $(0.5 \cdot n^{mom})$ and increased $(1.25 \cdot n_{rnom})$ speed for two cases:

- 1. In the absence of eccentricity;
- 2. In the presence of eccentricity.

When conducting a study with rotor eccentricity, the value of the rotor eccentricity modulation coefficient was chosen to be $\gamma \ge 10\%$. The modeling of the presence of eccentricity was carried out in accordance with the algorithm given in [36].

As a result of the modeling, the following time diagrams of the phase currents of the stator of an induction motor in steady state were obtained:

- 1. Reduced speed in the absence (Fig. 3, a) and in the presence (Fig. 3, b) of eccentricity.;
- 2. Nominal speed in the absence (Fig. 4, a) and in the presence (Fig. 4, b) of eccentricity.;
- 3. Iincreased speed in the absence (Fig. 5, a) and in the presence (Fig. 5, b) of eccentricity.



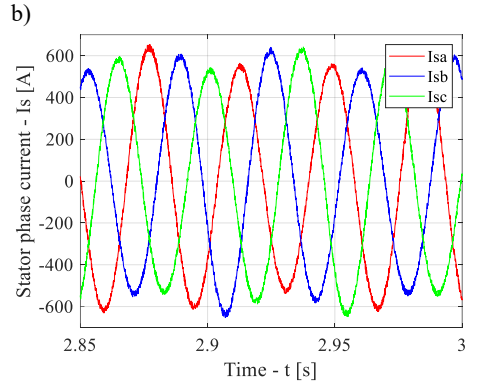


Fig. 3. Time diagrams of stator phase currents at reduced speed: eccentricity present (a) and absent (b)

Table 1. Parameters of the IM of the STA-1200 series [72, 73]

Parameter	Designation	Unit	Value
Nominal power	P_{nom}	kW	1,200
Nominal stator voltage frequency	f_{snom}	Hz	55.8
Nominal stator phase voltage	U_{smon}	V	1,080
Nominal stator phase current	I_{snom}	A	450
Nominal rotor speed	n_r	rpm	1,110
Number of pole pairs	p	r. u.	3
Moment of inertia	J	kg⋅m²	39

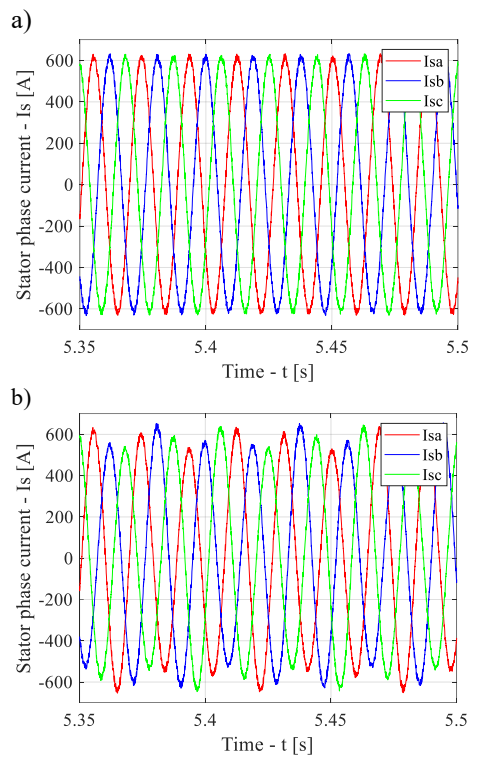


Fig. 4. Time diagrams of stator phase currents at the nominal speed: eccentricity present (a) and absent (b)

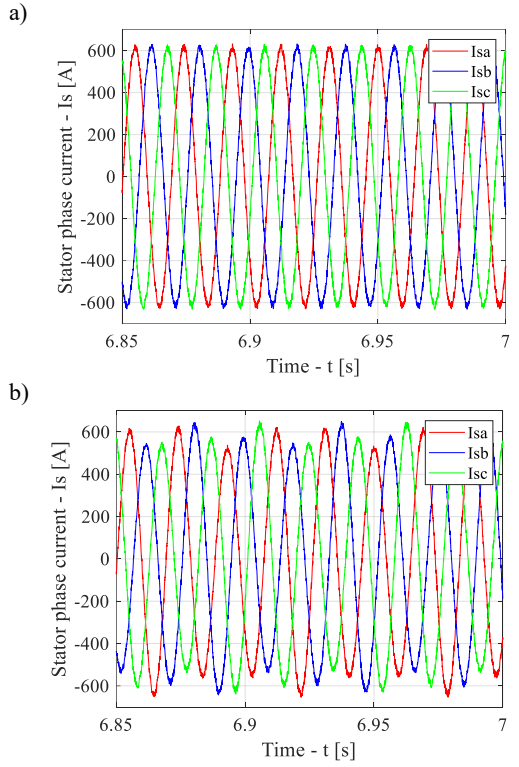


Fig. 5. Time diagrams of stator phase currents at the increased speed: eccentricity present (a) and absent (b)

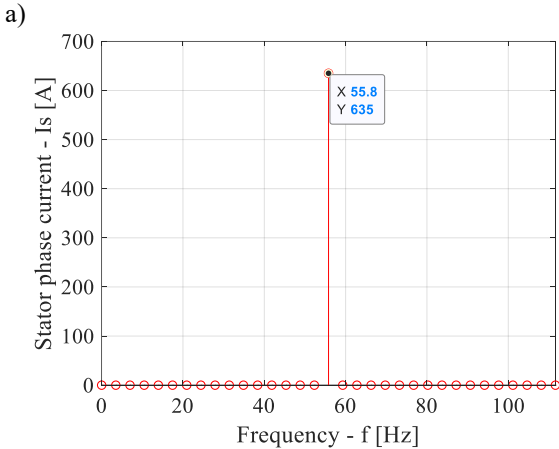
For the time diagrams shown in Fig. 3-Fig. 5, the AFS of the stator phase currents were calculated and constructed, determined using the fast Fourier transform (FFT) and using the proposed Prony method.

When using the FFT, the frequencies of the stator phase current signals obtained from the FOC were used.

Since there are no asymmetric winding modes in the IM, the calculations of the spectra of the stator phase current signals were carried out only for phase A.

As a result of the research, the following amplitudefrequency spectra of the stator current of phase A of the induction motor were obtained:

- 1. At a reduced speed in the absence of eccentricity, determined using the FFT (Fig. 6, a) and using the proposed Prony method (Fig. 6, b).;
- 2. At a reduced speed in the presence of eccentricity, determined using the FFT (Fig. 7, a) and using the proposed Prony method (Fig. 7, b);
- 3. At the nominal speed in the absence of eccentricity, determined using the FFT (Fig. 8, a) and using the proposed Prony method (Fig. 8, b);
- 4. At the nominal speed in the presence of eccentricity, determined using the FFT (Fig. 9, a) and using the proposed Prony method (Fig. 9, b);
- 5. At an increased speed in the absence of eccentricity, determined using the FFT (Fig. 10 a) and using the proposed Prony method (Fig. 10, b);
- 6. At an increased speed in the presence of eccentricity, determined using the FFT (Fig. 11, a) and using the proposed Prony method (Fig. 11, b).



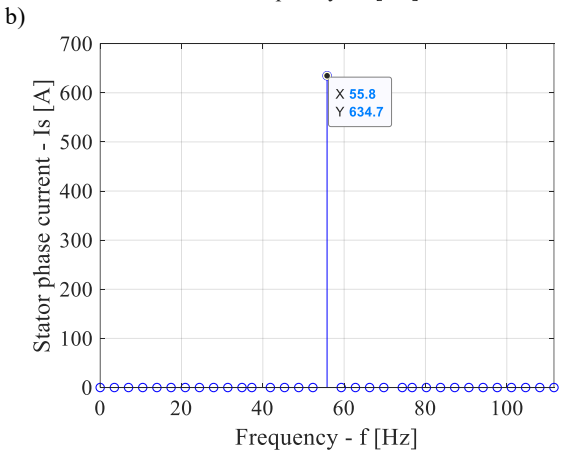


Fig. 6. AFS of the stator current of phase A of an IM at a reduced speed in the absence of eccentricity, determined using the FFT (a) and using the proposed Prony method (b)

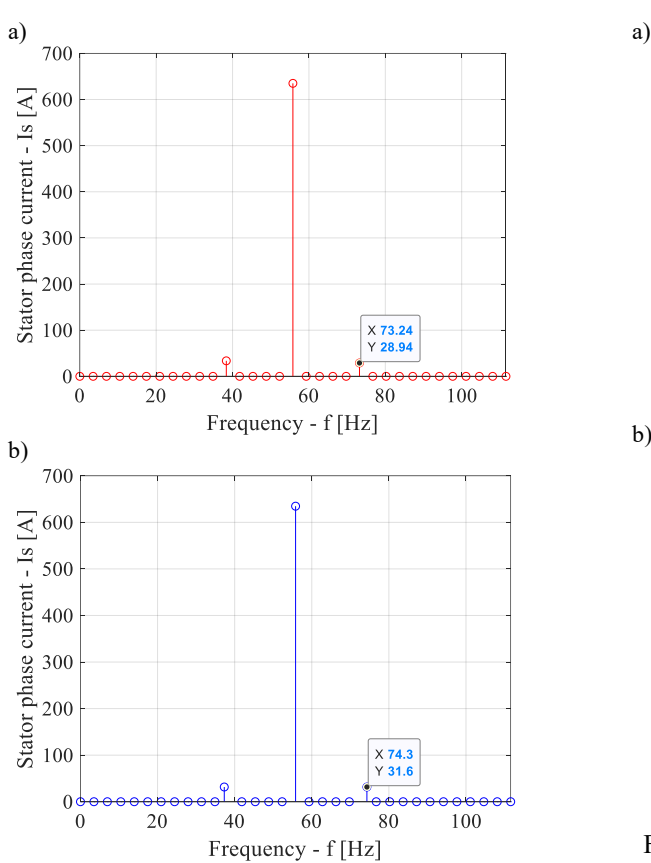
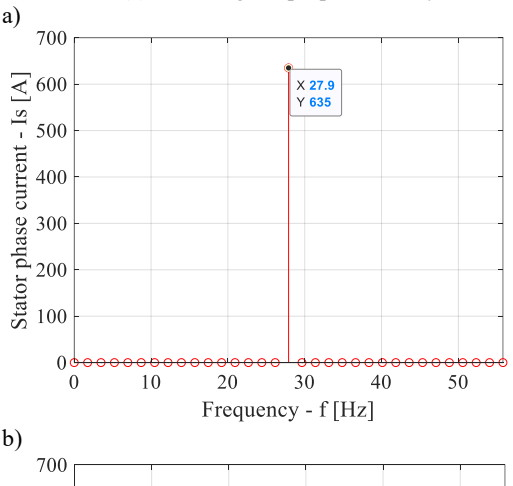


Fig. 7. AFS of the stator current of phase A of an IN at a speed in the presence of rotor eccentricity, determined using the FFT (a) and using the proposed Prony method (b)



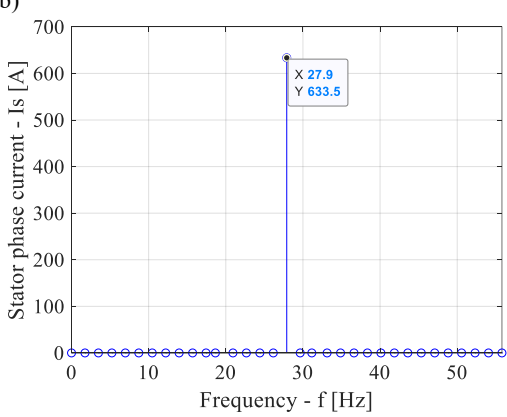
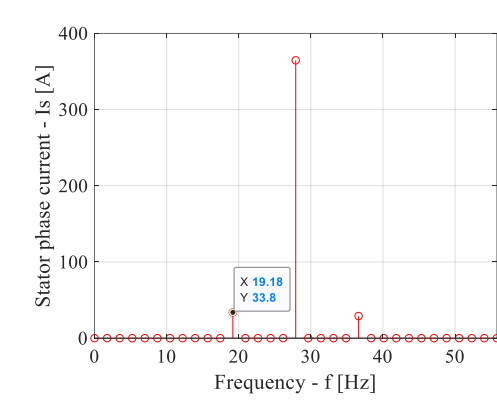


Fig. 8. AFS of the stator current of phase A of an IM at the rated speed in the absence of eccentricity, determined using the FFT (a) and using the proposed Prony method (b)



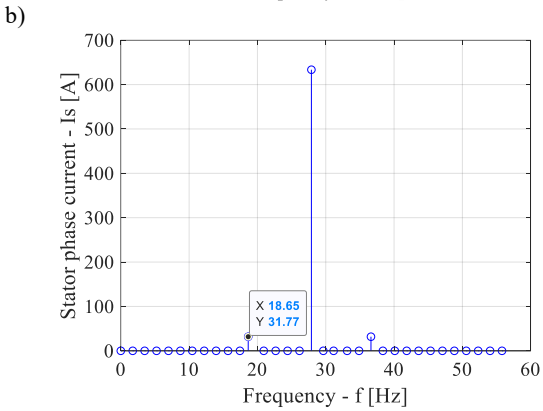
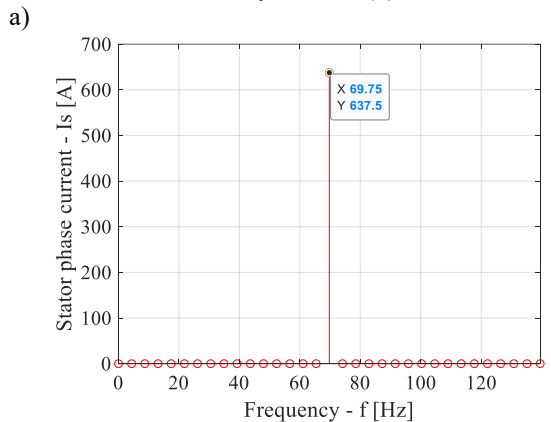


Fig. 9. AFS of the stator current of phase A of an IM at the rated speed in the presence of eccentricity, determined using the FFT (a) and using the proposed Prony method (b)



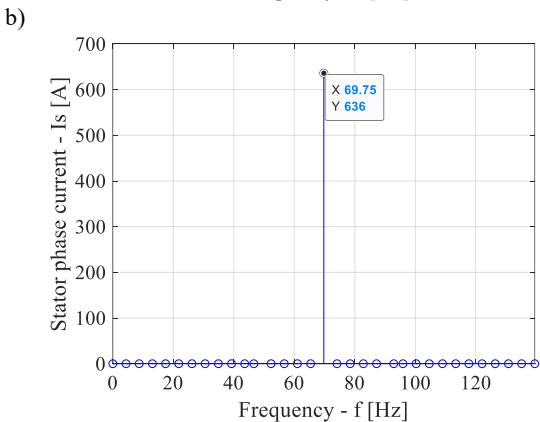
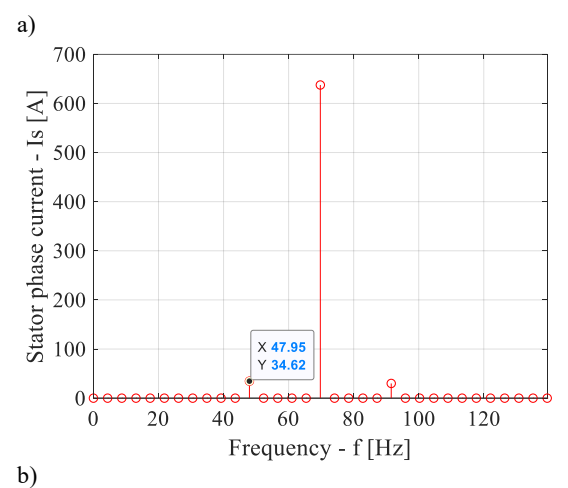


Fig. 10. AFC of the stator current of phase A of an IN at an increased speed in the absence of eccentricity, determined using the FFT (a) and using the proposed Prony method (b)



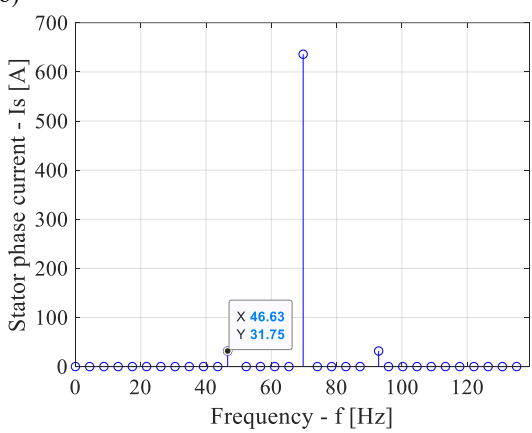


Fig. 11. AFS of the stator current of phase A of an IM at an increased speed in the presence of eccentricity, determined using the FFT (a) and using the proposed Prony method (b)

4.3. Discussion of the results

From the time diagrams (Fig. 7, Fig. 9, Fig. 11) the values of the harmonics of the subsynchronous type of the amplitude-frequency spectral components of the phase currents of the stator of the IM, located to the left (L) and to the right (R) relative to the fundamental frequency, were obtained. The results are listed in Table 2

According to formula (24), the values of the subsynchronous type harmonics of the amplitude-frequency spectra of the phase currents of the stator of an IM are calculated. These are the values of the amplitudes of the subsynchronous type harmonics of

the stator phase currents. The results are listed in Table 2.

The values of the amplitudes of the subsynchronous type harmonics and the corresponding components of the AFS of the phase currents of the stator of an IM, obtained using the FFT and the proposed Prony method, were compared. The errors in determining the spectral components of the subsynchronous type are listed in Table 2.

From the analysis of the results given in Table 2, it follows that the values of the errors in determining the spectral components of the subsynchronous type, obtained using the proposed Prony method, are smaller than the values of the errors in determining the spectral components of the subsynchronous type, obtained using the fast Fourier transform.

In addition, when using the proposed Prony method, the values of the left and right spectral components of the subsynchronous type are the same.

However, when using the FFT, the values of the left and right spectral components of the subsynchronous type are different. This fact may lead to ambiguity in determining the degree of eccentricity.

Analysis of the results shown in Fig. 6, b-11, b and expression (24) allows us to conclude that the eccentricity modulation coefficient γ is directly proportional to the degree of eccentricity. Therefore, it can be a criterion for determining the degree of damage to an induction motor.

Despite the fact that vibration diagnostics methods are well developed and have high accuracy, their use in building an operational diagnostics system will give incorrect results. This is due to the fact that vibrations caused by operational factors will be present in the traction drive, which will have a negative impact on the diagnostic results.

As noted above, the value of static eccentricity is much greater than dynamic. Dynamic eccentricity has the same diagnostic symptoms as static. When diagnosing, it does not matter what type of eccentricity is present in the asynchronous motor. Therefore, the work considered only cases when only static eccentricity is present in the induction motor.

The work considered an asynchronous motor with a squirrel-cage rotor. Expression (24) and the nature of the results shown in Fig. 6, b - 11, b will be valid for asynchronous motors with a phase rotor. In addition,

Table 2. Analysis of the accuracy of determining the values of harmonics of the subsynchronous type of AFS of the stator phase currents of an IM

	Methods									
Motor shaft speed _	Calculation by formula (24)	Fa	ast Fourie	er transfor	m	Pro	Prony proposed method			
	I_{sA} , A	L		R		L		R		
		I'_{sAl} , A	σ'_l , %	I'_{sAr} , A	σ' _r , %	I''_{sAl} , A	σ" _l , %	I''_{sAr} , A	σ" _r , %	
Reduced	31.82	33.62	5.66	28.94	9.1	31.6	0.7	31.6	0.7	
Nominal	31.82	33.8	6.22	29.04	8.74	31.77	0.16	31.77	0.16	
Increased	31.82	34.62	8.8	29.94	5.91	31.75	0.22	31.75	0.22	

the proposed method may be valid for such types of AC motors as synchronous. For DC motors, the proposed approach to determining the presence of eccentricity may also be theoretically valid. But for both the case of synchronous and DC motors, additional research should be conducted.

The validity of the proposed method in diagnosing the presence of eccentricity in the specified types of electric motors is due to the fact that in the absence of eccentricity, the rotating field at all points in space at the same distance from the geometric center of the stator of the electric motor will be the same. And the presence of eccentricity causes a shift of the geometric centers of the stator and rotor of the electric motor. This will lead to the appearance of additional spectral components in the electric motor currents.

The need for additional research to apply the proposed method in diagnosing the presence of eccentricity in the specified types of electric motors is due to the fact that in synchronous motors there is no rotor slip, and in DC motors the current value (in the absence of eccentricity) is constant. Therefore, the expression for determining the frequencies of subsynchronous type harmonics (23) is incorrect, and therefore the expression (24) will also be incorrect.

The establishment of analytical expressions for determining the frequencies of subsynchronous harmonics in the presence of eccentricity in synchronous motors and DC motors is an urgent task for individual studies.

5. CONCLUSION

This paper considers a method for increasing the efficiency of diagnosing rotor eccentricity in IM by combining the Prony method and the algorithm for implementing the Wiener-Hopf theorem. The proposed solution allows improving the quality of diagnosing defects of mechanical origin that cause eccentricity by reducing the influence of noise, compensating for variable load modes, and eliminating ambiguities when choosing the model order. Unlike traditional analysis of the current spectrum using the FFT, the Prony method provides a more accurate estimate of the amplitudes of subsynchronous harmonics, which are directly related to the degree of eccentricity. It is worth noting that subsynchronous-type located harmonics, symmetrically (left and right) relative to the fundamental frequency, are characterized by the same amplitude values, which increases the accuracy of diagnostic results and eliminates determinations of the degree of eccentricity. The modeling conducted on the example of the STA-1200 motor confirmed the advantages of the proposed approach in the presence of thermal noise and changes in the rotational speed. Thus, the proposed system has an innovative approach to the problems of increasing the accuracy of operational diagnostics of traction motor defects and can be recommended as a basis for creating or improving on-board diagnostic systems with the detection of defects that cause eccentricity at the early operation stages of electric drives of railway transport.

Further research will be aimed at developing a structural diagram of an embedded eccentricity monitoring system with connection to the on-board control network of the diagnostic system. Separate studies are also planned to be devoted to taking into account transient modes: starting, braking, reversing, which are characteristic of traction drives.

Source of funding: This research received no external funding.

Author contributions: research concept and design, S.G., O.G.; Collection and/or assembly of data, S.G., V.Y, O.P. V.S.; Data analysis and interpretation, S.G., O.G., V.Y., O.P.; Writing the article, S.G., O.G., V.Y., O.P., V.S.; Critical revision of the article, O.G.; Final approval of the article, S.G.

Declaration of competing interest: The authors declare that they have no known competing financial interests or personal relationships that could have appeared to influence the work reported in this paper.

REFERENCES

- Polater N, Tricoli P. Technical review of traction drive systems for light railways. Energies. 2022;15(9);3187. https://doi.org/10.3390/en15093187.
- Sulym A, Khozia P. Analysis of management strategies for energy exchange processes in the electric rolling stock with on-board capacitive energy storages. 2021 IEEE 2nd KhPI Week on Advanced Technology (KhPIWeek). 2021:109-114. https://doi.org/10.1109/KhPIWeek53812.2021.9569992.
- 3. Ronanki D. Overview of rolling stock. Transportation Electrification: Breakthroughs in Electrified Vehicles. Aircraft, Rolling Stock, and Watercraft. 2022:249-281. https://doi.org/10.1002/9781119812357.ch11.
- Issa R, Clerc G, Hologne-Carpentier M, Michaud R, Lorca E, Magnette C, Messadi A. Review of fault diagnosis methods for induction machines in railway traction applications. Energies. 2024;17(11):2728. https://doi.org/10.3390/en17112728.
- Liubarskyi BG, Overianova LV, Riabov IS, Iakunin DI, Ostroverkh OO, Voronin YV. Estimation of the main dimensions of the traction permanent magnet-assisted synchronous reluctance motor. Electrical Engineering & Electromechanics. 2021;(2):3–8. https://doi.org/10.20998/2074-272X.2021.2.01.
- 6. Wang J, Ren C, Liu Z, Mao M. Research on direct drive technology of the permanent magnet synchronous motor for urban rail vehicles. Mathematical Problems in Engineering. 2022;(1):8312121. https://doi.org/10.1155/2022/8312121.
- 7. Hu H, Liu Y, Li Y, He Z, Gao S, Zhu X, Tao H. Traction power systems for electrified railways: evolution, state of the art, and future trends. Railway Engineering Science. 2024;32(1):1-19. https://doi.org/10.1007/s40534-023-00320-6.
- Domínguez M, Fernández-Cardador A, Fernández-Rodríguez A, Cucala AP, Pecharromán RR, Sánchez PU, Cortázar IV. Review on the use of energy storage systems in railway applications. Renewable and Sustainable Energy Reviews. 2025;207:114904.

- https://doi.org/10.1016/j.rser.2024.114904.
- Akay ME, Ustaoglu A. Energetic, exergetic, and environmental evaluation of railway transportation by diesel and electric locomotives. Environmental Progress & Sustainable Energy. 2022;41(3):e13804. https://doi.org/10.1002/ep.13804.
- 10. Chen Z. Analysis the principle and applications for locomotive engine. Applied and Computational Engineering. 2024;98:47-51. https://doi.org/10.54254/2755-2721/98/2024FMCEAU0111.
- Riabov I, Yeritsyan B, Roi S, Kachan A. Determination of the rational strategy of voltage regulation of the traction induction electric motor for a shunting diesel locomotive with a group-driven wheelsets. Engineering Research Express. 2025. https://doi.org/10.1088/2631-8695/add1af.
- Sulym AO, Fomin OV, Khozia PO, Mastepan AG. Theoretical and practical determination of parameters of on-board capacitive energy storage of the rolling stock Naukovyi Visnyk Natsionalnoho Hirnychoho Universytetu. 2018;(5):79-87. https://doi.org/10.29202/nvngu/2018-5/8.
- 13. Fomin O, Sulym A, Kulbovskyi I, Khozia P, Ishchenko V. Determining rational parameters of the capacitive energy storage system for the underground railway rolling stock. Eastern-European Journal of Enterprise Technologies. 2018;21(92):63–71. https://doi.org/10.15587/1729-4061.2018.126080.
- Abouzeid AF, Guerrero JM, Vicente-Makazaga I, Muniategui-Aspiazu I, Endemaño-Isasi A, Briz F. Torsional vibration suppression in railway traction drives. IEEE Access. 2022;10;32855-32869. https://doi.org/10.1109/ACCESS.2022.3162415.
- Vantagodi NV, Abouzeid AF, Guerrero JM, Vicente-Makazaga I, Muniategui-Aspiazu I, Endemaño-Isasi A, Briz F. Design of a scaled roller-rig test bench for antislip control development for railway traction. IEEE Transactions on Vehicular Technology. 2022;72(4): 4320-4331. https://doi.org/10.1109/TVT.2022.3226607.
- Goolak S, Liubarskyi B. Vector control system taking into account the saturation of an induction motor. Tehnički Vjesnik. 2024;31(4):1170-1178. https://doi.org/10.17559/TV-20221015124239.
- 17. Wang X, Wang J, Yang J, Yao D, Zhao Y, Chen B. Dynamic characteristics of electromechanical coupling of body-suspended drive system for high-speed trains under wheel polygonal wear. Transactions of the Canadian Society for Mechanical Engineering. 2024;48(4):659-670. https://doi.org/10.1139/tcsme-2024-0056.
- Goolak S, Liubarskyi B, Riabov I, Chepurna N, Pohosov O. Simulation of a direct torque control system in the presence of winding asymmetry in induction motor. Engineering Research Express. 2025;5:025070-025086. http://doi.org/10.1088/2631-8695/acde46.
- Gerlici J, Lovska A, Vatulia G, Pavliuchenkov M, Kravchenko O, Solcansky S. Situational adaptation of the open wagon body to container transportation. Applied Sciences. 2023;13(15):8605. https://doi.org/10.3390/app13158605.
- Vatulia GL, Lovska AO, Krasnokutskyi YS. Research into the transverse loading of the container with sandwich-panel walls when transported by rail. In IOP Conference Series: Earth and Environmental Science. 2023;1254(1):012140. https://doi.org/10.1088/1755-1315/1254/1/012140.
- 21. Lovska A, Gerlici J, Dizo J, Ishchuk V. The strength of rail vehicles transported by a ferry considering the

- influence of sea waves on its hull. Sensors. 2024;24:183. https://doi.org/10.3390/s24010183.
- 22. Gubarevych O, Goolak S, Daki O, Yakusevych Y. Determining an additional diagnostic parameter for improving the accuracy of assessment of the condition of stator windings in an induction motor. Eastern-European Journal of Enterprise Technologies. 2021;5(113):21–29. http://doi.org/10.15587/1729-4061.2021.239509.
- Goolak S, Liubarskyi B, Lukoševičius V, Keršys R, Keršys A. Operational diagnostics system for asymmetric emergency modes in traction drives with direct torque control. Applied Sciences. 2023;13(9):5457. https://doi.org/10.3390/app13095457.
- 24. Gubarevych O, Goolak S, Golubieva S. Systematization and selection of diagnosing methods for the stator windings insulation of induction motors. Rev. Roum. Sci. Techn. Électrotechn. et Énerg. 2022;67(4):445-450.
- Yousuf M, Alsuwian T, Amin AA, Fareed S, Hamza M. IoT-based health monitoring and fault detection of industrial AC induction motor for efficient predictive maintenance. Measurement and Control. 2024;57(8): 1146-1160. https://doi.org/10.1177/00202940241231473.
- Hassan IU, Panduru K, Walsh J. An in-depth study of vibration sensors for condition monitoring. Sensors. 2024;24(3):740. https://doi.org/10.3390/s24030740.
- Konda YR, Ponnaganti VK, Reddy PVS, Singh RR, Mercorelli P, Gundabattini E, Solomon DG. Thermal analysis and cooling strategies of high-efficiency threephase squirrel-cage induction motors - A review. Computation. 2024;12(1):6. https://doi.org/10.3390/computation12010006.
- García-Pérez D, Saeed M, Díaz I, Enguita JM, Guerrero JM, Briz F. Machine learning for inverter-fed motors monitoring and fault detection: An overview. IEEE Access. 2024;12:27167-27179. https://doi.org/10.1109/ACCESS.2024.3366810.
- 29. Gubarevych O, Goolak S, Daki O, Tryshyn V. Investigation of turn-to-turn closures of stator windings to improve the diagnostics system for induction motors. Problemele Energeticii Regionale. 2021;2(50):10-24. https://doi.org/10.52254/1857-0070.2021.2-50.02.
- 30. Kryvonosov V, Matvienko O, Antipov I, Stefani B, Zaporozhets A, Borychenko O, Cherniavskyi A. Nondestructive test method for diagnosing turn-to-turn circuits of electric motor windings under conditions of local reactive power compensation. Modern Technologies in Energy and Transport II. 2025:281-297. https://doi.org/10.1007/978-3-031-76650-3 15.
- 31. Gubarevych O, Gerlici J, Gorobchenko O, Kravchenko K, Zaika D. Analysis of the features of application of vibration diagnostic methods of induction motors of transportation infrastructure using mathematical modelling. Diagnostyka. 2023;24(1):1-10. https://doi.org/10.29354/diag/161308.
- 32. Goolak S, Gubarevych O, Gorobchenko O, Nevedrov O, Kamchatna-Stepanova K. Investigation of the influence of the quality of the power supply system on the characteristics of an asynchronous motor with a squirrel-cage rotor. Przeglad Elektrotechniczny. 2022;98(6):142–148. http://doi.org/10.15199/48.2022.06.26-
- 33. Gerlici J, Goolak S, Gubarevych O, Kravchenko K, Kamchatna-Stepanova K, Toropov A. Method for determining the degree of damage to the stator windings of an induction electric motor with an asymmetric power system. Symmetry. 2022;14(7):1305. https://doi.org/10.3390/sym14071305.
- 34. Gubarevych O, Wierzbicki S, Petrenko O, Melkonova I, Riashchenko O. Modular unit for monitoring of elements

- of asynchronous machine for improving reliability during operation. Diagnostyka. 2024;25(4):2024411. https://doi.org/10.29354/diag/194688.
- 35. Goolak S, Gorobchenko O, Holub H, Dudnyk Y. Increasing the efficiency of railway rolling stock operation with induction traction motors due to implementation of the operational system for diagnostic condition of rotor. Diagnostyka. 2024;25(4):1-11. https://doi.org/10.29354/diag/193809.
- Goolak S, Gubarevych O, Yurchenko V, Kyrychenko M. A review of diagnostic information processing methods in the construction of systems for operating diagnostics of rotor eccentricity of induction motors. Diagnostyka. 2025; 26(1): 1-15. https://doi.org/10.29354/diag/202757.
- Zhou L, Wang B, Lin C, Inoue H, Miyoshi M. Static eccentricity fault detection for psh-type induction motors considering high-order air gap permeance harmonics. In 2021 IEEE International Electric Machines & Drives Conference (IEMDC). 2021:1-7. https://doi.org/10.1109/IEMDC47953.2021.9449496.
- Garcia-Calva T, Morinigo-Sotelo D, Fernandez-Cavero V, Romero-Troncoso R. Early detection of faults in induction motors A review. Energies. 2022;15(21): 7855. https://doi.org/10.3390/en15217855.
- Petryna J, Duda A, Sułowicz M. Eccentricity in induction machines - A useful tool for assessing its level. Energies. 2021;14(7):1976. https://doi.org/10.3390/en14071976.
- Viswanath S, Praveen Kumar N, Isha TB. Static eccentricity fault in induction motor drive using finite element method. In Advances in Electrical and Computer Technologies: Select Proceedings of ICAECT 2019. 2020:1291-1302. https://doi.org/10.1007/978-981-15-5558-9 108.
- 41. Liu Z, Zhang P, He S, Huang J. A review of modeling and diagnostic techniques for eccentricity fault in electric machines. Energies. 2021;14(14):4296. https://doi.org/10.3390/en14144296.
- 42. Widagdo RS, Hermawati FA, Hariadi B. Unbalanced voltage detection with measurement current signature analysis (MCSA) in 3-phase induction motor using Fast Fourier Transform (FFT). Jurnal Teknologi Elektro. 2024;15(02):95-101. https://doi.org/10.22441/jte.2024.v15i2.003.
- 43. Deeb M, Kotelenets NF. Fault diagnosis of 3-phase induction machine using harmonic content of stator current spectrum. 2020 International Youth Conference on Radio Electronics, Electrical and Power Engineering (REEPE). 2020:1-6. https://doi.org/10.1109/REEPE49198.2020.9059213.
- 44. Krishnasarma A, Mostafavi Yazdi SJ, Taylor A, Ludwigsen D, Baqersad J. Acoustic signature analysis and sound source localization for a three-phase AC induction motor. Energies. 2021;14(21):7182. https://doi.org/10.3390/en14217182.
- 45. Allal A, Khechekhouche A. Diagnosis of induction motor faults using the motor current normalized residual harmonic analysis method. International Journal of Electrical Power & Energy Systems. 2022;141:108219. https://doi.org/10.1016/j.ijepes.2022.108219.
- 46. Chen X, Feng Z. Order spectrum analysis enhanced by surrogate test and Vold-Kalman filtering for rotating machinery fault diagnosis under time-varying speed conditions. Mechanical Systems and Signal Processing. 2021;154:107585. https://doi.org/10.1016/j.ymssp.2020.107585.
- 47. Chehaidia SE, Cherif H, Alraddadi M, Mosaad MI, Bouchelaghem AM. Experimental diagnosis of broken rotor bar faults in induction motors at low slip via hilbert envelope and optimized subtractive clustering adaptive

- neuro-fuzzy inference system. Energies. 2022;15(18): 6746. https://doi.org/10.3390/en15186746.
- 48. Guezam A, Bessedik SA, Djekidel R. Fault diagnosis of induction motors rotor using current signature with different signal processing techniques. Diagnostyka. 2022;23(2):1-9. https://doi.org/10.29354/diag/147462.
- Gangsar P, Tiwari R. Signal based condition monitoring techniques for fault detection and diagnosis of induction motors: A state-of-the-art review. Mechanical Systems and Signal Processing. 2020;144:106908. https://doi.org/10.1016/j.ymssp.2020.106908.
- Frosini L. Novel diagnostic techniques for rotating electrical machines - A review. Energies. 2020;13(19):5066. https://doi.org/10.3390/en13195066.
- Abdellah C, Mama C, Meflah Abderrahmane MR, Mohammed B. Current Park's vector pattern technique for diagnosis of broken rotor bars fault in saturated induction motor. Journal of Electrical Engineering & Technology. 2023;18(4):2749-2758. https://doi.org/10.1007/s42835-022-01342-6.
- 52. Kahraman E, Ulusoy AE, Şerifoğlu MO, Kara DB. Park vector approach based misalignment detection strategy for IMs. 14th International Conference on Electrical and Electronics Engineering (ELECO). 2023:1-5. https://doi.org/10.1109/ELECO60389.2023.10416077.
- Laadjal K, Sahraoui M, Alloui A, Cardoso AJM. Threephase induction motors online protection against unbalanced supply voltages. Machines. 2021;9(9):203. https://doi.org/10.3390/machines9090203.
- 54. Chen X, Feng Z. Tacholess speed estimation for rotating machinery fault diagnosis of induction motor drivetrain. IEEE Transactions on Power Electronics. 2024;39(4): 4704-4713. https://doi.otg/10.1109/TPEL.2023.3349138.
- 55. Laadjal K, Cardoso AJM, Sahraoui M, Alloui A. A novel stator faults indicator in three-phase induction motors, based on voltage and impedance symmetrical components. IECON 2022–48th Annual Conference of the IEEE Industrial Electronics Society. 2022;1-6. https://doi.org/10.1109/IECON49645.2022.9968349.
- Lee CY, Huang KY, Jen LY, Zhuo GL. Diagnosis of Defective rotor bars in induction motors. Symmetry. 2020;12(11):1753. https://doi.org/10.3390/sym12111753.
- Kumar RR, Andriollo M, Cirrincione G, Cirrincione M, Tortella A. A comprehensive review of conventional and intelligence-based approaches for the fault diagnosis and condition monitoring of induction motors. Energies. 2022;15(23):8938. https://doi.org/10.3390/en15238938.
- 58. Kim MC, Lee JH, Wang DH, Lee IS. Induction motor fault diagnosis using support vector machine, neural networks, and boosting methods. Sensors. 2023;23(5): 2585. https://doi.org/10.3390/s23052585.
- 59. Niu H, Chen Y. Why do big data and machine learning entail the fractional dynamics? In Smart big data in digital agriculture applications: acquisition, advanced analytics, and plant physiology-informed artificial intelligence, 2023:15-53. Cham: Springer Nature Switzerland. https://doi.org/10.1007/978-3-031-52645-9 2.
- 60. Nigmatullin RR, Sabatier J. How to detect and fit "fractal" curves, containing power-law exponents? Part 2. In 2023 International Conference on Fractional Differentiation and Its Applications (ICFDA. 2023:1-5. https://doi.org/10.1109/ICFDA58234.2023.10153375
- Nigmatullin RR, Lino P, Maione G. The statistics of fractional moments and its application for quantitative reading of real data. New Digital Signal Processing Methods: Applications to Measurement and Diagnostics, 2020:87;139. https://doi.org/10.1007/978-3-030-45359-6

- 62. Huang Y, Wang H, Yin H, Zhao Z. Iterative time-varying channel prediction based on the vector prony method. Wireless Personal Communications. 2024;136(1):103-122. https://doi.org/10.1007/s11277-024-11162-8.
- 63. Kaur J, Parmar KS, Singh S. Autoregressive models in environmental forecasting time series: a theoretical and application review. Environmental Science and Pollution Research. 2023;30(8):19617-19641. https://doi.org/10.1007/s11356-023-25148-9.
- 64. Menin B. Objective model selection in physics: Exploring the finite information quantity approach. Journal of Applied Mathematics and Physics. 2024; 12(5):1848-1889. https://doi.org/10.4236/jamp.2024.125115.
- 65. Ding J, Tarokh V, Yang Y. Bridging AIC and BIC: a new criterion for autoregression. IEEE Transactions on Information Theory. 2017;64(6):4024-4043. https://doi.org/10.1109/TIT.2017.2717599.
- 66. Lin WC, Tsai CF, Zhong JR. Deep learning for missing value imputation of continuous data and the effect of data discretization. Knowledge-Based Systems. 2022;239: 108079. https://doi.org/10.1016/j.knosys.2021.108079.
- 67. Li H. Time-series analysis. In Numerical Methods Using Kotlin: For Data Science. Analysis, and Engineering. 2022:737-881. https://doi.org/10.1007/978-1-4842-8826-9 15.
- Macedo P. A two-stage maximum entropy approach for time series regression. Communications in Statistics-Simulation and Computation. 2024;53(1):518-528. https://doi.org/10.1080/03610918.2022.2057540.
- 69. Subba Rao S, Yang J. A prediction perspective on the Wiener–Hopf equations for time series. Journal of Time Series Analysis. 2023;44(1):23-42. https://doi.org/10.1111/jtsa.12648.
- Goolak S, Liubarskyi B, Sapronova S, Tkachenko V, Riabov I. Refined model of asynchronous traction electric motor of electric locomotive. Transport Means -Proceedings of the International Conference. 2021:455– 460
- Goolak S, Riabov I, Petrychenko O, Kyrychenko M, Pohosov O. The simulation model of an induction motor with consideration of instantaneous magnetic losses in steel. Advances in Mechanical Engineering. 2025;17(2): 16878132251320236.

https://doi.org/10.1177/16878132251320236.



Sergey GOOLAK. Candidate of Technical Sciences, Associate Professor Department of Electromechanics and Rolling Stock of Railways of National Transport University, Kyiv, Ukraine. Scientific interests – technical diagnostics of drives of transport systems.

E-mail: sgoolak@gmail.com



Oleg GUBAREVYCH. Candidate of technical sciences, Associate Professor, Corresponding Member of the Academy of Applied Sciences, Department of Electromechanics and Rolling Stock of Railways. Educational and Scientific Kyiv Institute of Railway Transport, National Transport University, Kyiv, Ukraine. The main research is aimed

at improving reliability and developing diagnostic methods for electrical equipment.

E-mail: <u>oleg.gbr@ukr.net</u>



Vasyl SAVYK. Candidate Technical Sciences, Associate Professor of the Department of Oil Engineering Gas Technologies of the National "Yuriy University Kondratyuk Poltava Polytechnic". Scientific interests - mathematical modeling of thermodynamic processes.



Victor YURCHENKO.

E-mail: savycvasyl@ukr.net

Postgraduate, Department of Electromechanics and Rolling Stock of Railways of National Transport University, Kyiv, Ukraine. Scientific interests – methods of diagnosing induction motors.

E-mail: vitekshef1997@gmail.com



Oleksandr POHOSOV. Candidate of Technical Sciences, Kyiv National University of Construction and Architecture. Field of scientific interests – mathematical modeling of thermodynamic processes.

E-mail: <u>pogosov_aleksandr@ukr.net</u>